Cellulose (2021) 28:1663–1686
https://doi.org/10.1007/s10570-020-03641-5

ORIGINAL RESEARCH

Micro-structure and mechanical properties of microcrystalline cellulose-sisal fiber reinforced cementitious composites developed using cetyltrimethylammonium bromide as the dispersing agent

Aloysio Souza Filho · Shama Parveen · Sohel Rana · Romel Vanderlei · Raul Fangueiro

Received: 13 September 2020 / Accepted: 15 December 2020 / Published online: 6 January 2021

Abstract This paper reports new hierarchical cementitious composites developed using microcrystalline cellulose (MCC), sisal fibers and cetyltrimethylammonium bromide (CTAB) as the dispersing agent. MCC was dispersed in water without and with CTAB at different concentrations using ultrasonication and the optimum CTAB concentration for achieving homogeneous and stable MCC suspensions was found to be 40%. Hierarchical composites were fabricated using MCC (0.1–1.5 wt% of cement), sisal fibers (20 mm, 0.25% and 0.50 wt% of cement), 40% CTAB and tri-butyl phosphate as the defoaming agent. Mechanical strengths of composites improved significantly at 0.1 wt% MCC, which along with 0.5% sisal fibers improved compressive and flexural strengths by $\sim$ 24% and $\sim$ 18%, respectively. The hybrid reinforcement exhibited a synergistic effect on the fracture behavior of composites improving the fracture energy up to 40%. Hierarchical composites also showed improved fiber-matrix bonding, lower porosity and water absorption, superior hydration, carbonation resistance and durability up to 90 ageing cycles.

Keywords Cellulose · Reinforced cement/plaster · Fiber/matrix bond · Mechanical properties

A. S. Filho (✉)
Department of Civil Engineering, Federal University of Technology - Paraná - UTFPR, Apucarana Campus, Apucarana 86812-460, Brazil
e-mail: asouza@utfpr.edu.br

S. Parveen (✉) · S. Rana (✉)
School of Art, Design and Architecture, University of Huddersfield, Queensgate, Huddersfield HD1 3DH, UK
e-mail: parveenshama2011@gmail.com

S. Rana
e-mail: s.rana@hud.ac.uk

R. Vanderlei
Post Graduate Program in Civil Engineering (PCV), State University of Maringá – UEM, Maringá 87020-900, Brazil

R. Fangueiro
Department of Mechanical Engineering, University of Minho, Campus de Azurém, 4800-058 Guimarães, Portugal

R. Fangueiro
Centre for Textile Science and Technology, University of Minho, Campus de Azurém, 4800-058 Guimarães, Portugal

Introduction

Concrete is the most widely used construction material in buildings, bridges and infrastructures due its adaptability and low cost (Brandt 2008). It is a composite material composed of a cement matrix reinforced with fine and coarse aggregates (Brandt 2008). Cement is produced in more than 150 countries and the global production capacity of cement was 4200 million tons in 2016 (International Energy Agency 2020). However, the major disadvantage of concrete is its low tensile strength and fracture toughness (Brandt 2008). Its brittleness and susceptibility to crack formation and degradation reduce its performance and durability, requiring frequent maintenance and increasing its vulnerability towards natural disasters (Parveen et al. 2015). The incorporation of plant-based fibers into cementitious composites was found to be an effective and low cost solution for improving brittle nature of cementitious composites (Onésippe et al. 2010; Fu et al. 2017). Plant fibers such as sisal, hemp, jute, etc. can delay or prevent crack propagation in cementitious composites due to their crack-bridging ability (Onésippe et al. 2010; Fu et al. 2017). Besides available abundantly and low-cost, plant fibers present important environmental benefits as compared to synthetic fibers and metals and is, therefore, a more sustainable reinforcement for concrete. A number of studies demonstrated that short and randomly distributed plant fibers could effectively improve toughness and ductility of cementitious composites by bridging cracks and sustaining a considerable amount of load even after the peak or failure stress (Savastano et al. 2009; Silva et al. 2009; Fan and Fu 2016). However, reductions of elastic modulus and strength of cementitious composites have been the major drawback of plant fiber reinforcements, limiting their application in construction (Fujiyama et al. 2014) Poor fiber-matrix bonding, problem in compaction, fiber aggregation, etc. were reported as the main reasons for increased porosity and inferior strength and stiffness of plant fiber-reinforced cementitious composites (Fujiyama et al. 2014).

A recently proposed approach to overcome above problems is to extract nano/macro-scale materials from plant fibers or plant-based cellulose and use them in the cementitious composites (Balea et al. 2019). These nano/micro structures such as nanocrystalline cellulose (NCC), nanofibrillated cellulose (NFC), microcrystalline cellulose (MCC), microfibrillated cellulose (MFC), etc. offer a high modulus and strength, high surface area, excellent bonding with cementitious matrices, good compaction and dense composite microstructure and consequently, significantly improved the mechanical properties of cementitious composites (Das et al. 2009; Parveen et al. 2017a; Balea et al. 2019; Hisseine et al. 2019; Tarchoun et al. 2019). Although a positive effect was observed by NFC on the toughness of cementitious composites (Haddad Kolour et al. 2020) probably due to its fibrillar structure with a high aspect ratio, CNC and MCC (due to their high stiffness and low aspect ratio) did not show any positive effect (or even deteriorated in some studies) on the toughness and ductility of cementitious composites (Parveen et al. 2017b, 2018). To overcome this, hierarchical cementitious composites have been developed more recently by combining two types of reinforcements, one of which improved the strength and stiffness (i.e. the pre-cracking mechanical behavior) whereas the other reinforcement enhanced the toughness and ductility (i.e. the post-cracking behavior) (Alshaghel et al. 2018; Cao et al. 2019). For example, a combination of carbon nanotubes (CNTs) with MCC was used to improve both pre and post-cracking mechanical behavior of cementitious composites, in which MCC mainly improved the stiffness and strength, whereas CNTs controlled the post-cracking fracture behavior through crack-bridging (Alshaghel et al. 2018). Although CNTs were proved to be an excellent reinforcing material for developing high-strength and ductile cementitious composites, their high cost, processing problems and toxicity limited their application in the construction industry. Due to this reason, the present research proposed a new hierarchical cementitious composite containing low-cost, less hazardous and renewable plant-based reinforcing materials, namely MCC and plant fibers, as an alternative to CNT-based cementitious composites.

MCC has recently attracted research attention as a reinforcement of polymeric and cementitious composites due to its high mechanical properties, low cost and commercial availability (Anju et al. 2016; Rehman et al. 2019; Mohan Bhasney et al. 2020). However, it was observed that the reinforcing capability of MCC in cementitious composites was strongly dependent on the MCC dispersion state (Gómez Hoyos et al. 2013; Parveen et al.

2017b, 2018). While direct mixing of MCC into cementitious composites (without any dispersion step) could not improve or even deteriorated the mechanical properties (Gómez Hoyos et al. 2013), MCC dispersion using mechanical stirring and ultrasonication resulted in 20.5% and 19.2% improvements in flexural strength and 19.8% and 51.4% improvements in compressive strengths, respectively (Silva et al. 2018; Parveen et al. 2018). Moreover, an improved MCC dispersion using a non-ionic surfactant such as Pluronic F-127 further improved the mechanical properties of cementitious composites (flexural and compressive strength improved by 31% and 66%, respectively) (Parveen et al. 2017b). Therefore, to improve the reinforcing ability of MCC in hierarchical composites, CTAB has been used for the first time for fabricating MCC-sisal hierarchical cementitious composites. CTAB is a cationic surfactant and it was selected in the present study as it can act by both steric stabilization and coulombic repulsion mechanisms (Eyley and Thielemans 2014).

To summarize, according to the extensive research carried out on plant fiber-reinforced cementitious composites, plant fibers could significantly improve the ductility of cementitious composites, but reduced the modulus and strength. Recently, a few studies, which used MCC for the reinforcement of cementitious composites, demonstrated that MCC could significantly improve modulus and strength, but reduced the fracture energy of cementitious composites. The development of hierarchical composites combining two types of reinforcements (such as MCC and CNTs) proved to be an effective approach of improving modulus, strength as well as ductility of cementitious composites and therefore, the present research focused on developing hierarchical composites based on sisal fibers and MCC. The concept of developing hierarchical composites using a cementitious matrix is relatively new (has been extensively studied in polymeric composites). The hierarchical composites developed using sisal fibers and MCC are based on bio-based, low-cost and eco-friendly reinforcements, but have been rarely studied in the literature. The concept of tailoring cementitious composite's properties (i.e. strength and ductility) through the synergistic effect of these macro–micro fiber reinforcements is also quite new. Moreover, CTAB was used for the first time in this research to improve MCC dispersion in hierarchical cementitious composites. As MCC dispersion is one of the most critical factors influencing composite properties, attempts were made to study the effect of this surfactant and optimize its concentration to enhance MCC dispersion and composite properties. In addition, this research made the first attempt of characterizing the durability (through accelerated aging test) of hierarchical cementitious composites. Although previous studies characterized the durability of sisal and other plant fiber-reinforced cementitious composites, no study has characterized the durability of MCC-reinforced or hierarchical cementitious composites. This was performed to investigate if the hierarchical reinforcement had any positive effect on the long-term performance of cementitious composites. A systematic study has been performed to investigate the influence of CTAB concentration on MCC dispersion for finding the optimum CTAB concentration. Also, the microstructure, porosity, hydration products, mechanical properties and durability of MCC-sisal hierarchical cementitious composites have been studied in detail.

Experimental

Raw materials

MCC (Avicel® PH-101, price 163€/kg) powder, CTAB and Pluronic F-127 were supplied by Sigma Aldrich (Portugal). The defoaming agent, Tri-butyl phosphate (TBP) was supplied by Acros Organics (Thermo Fischer Scientific) and Ordinary Portland Cement (OPC), CEM I 42.5 R (International standard: ASTM-C150, Type V) was supplied by Secil (Portugal). The standard sand, certified according to EN 196-1 standard, was purchased from Société Nouvelle du Littoral (France) and sisal fibers were supplied from Brazil (price: 1.4 €/kg). The supplied fibers were cut into 20 mm lengths for use in the cementitious composites and into 20 cm lengths for the pull-out testing. Essential properties of above raw materials and chemicals are listed in Table 1.

The morphology of MCC and sisal fibers was characterized by Scanning Electron Microscope (FEG-SEM, NOVA 200 Nano SEM, FEI, after a coating with 30 nm Au–Pd) and is shown in Fig. 1. It is evident from Table 1 and Fig. 1 that both MCC particle size and sisal fiber diameter were in the

Table 1 Properties of raw materials used for developing hierarchical cementitious composites

Material	Properties	Values
MCC (Avicel® PH-101)[a]	Particle size, Sauter diameter, shape	2 to 260 μm, 49 μm, larger fibrous rods to smaller irregular cuboids
	Moisture content and solid density	~ 3 wt%, 1.54 g/cm^3
Sisal fibres	Size	20 mm and 20 cm
Ordinary Portland Cement (CEM I 42.5 R)[b]	Product composition	95-100% clinker + 0-5% additional components
	Loss on ignition	≤ 5.0%
	Insoluble residue	≤ 5.0%
	Sulphur trioxide (SO_3)	≤ 4.0%
	Chloride (Cl^-)	≤ 0.1%
	Initial setting time	≥ 60 min
	Soundness	≤ 10 mm
	2 days compressive strength	≥ 20.0 MPa
	28 days compressive strength	≥ 42.5 MPa and ≤ 62.5 MPa
Sand (CEN-EN 196-1)[c]	Moisture and SiO_2 content	≤ 0.2%, ≥ 95%
	Particle size distribution	
	Square mesh size (mm)	Cumulative sieve residue
	2.00	0
	1.60	7 ± 5
	1.00	33 ± 5
	0.50	67 ± 5
	0.16	87 ± 5
	0.08	99 ± 1
CTAB[a]	Type	Cationic surfactant
	Average molecular weight, Critical micelle concentration (CMC), pH	364.5 g/mol, 0.92 to 1.0 mM, 6.0-7.5
Pluronic® F-127[a]	Type, molecular weight, CMC	Non-ionic, 12500 g/mol, 950-1000 ppm

[a]Source: Sigma Aldrich. [b]Source: www.secil.pt. [c]Source: www.tecnilab.pt

micron range; however, sisal fibers had lengths in millimeter scale (20 mm) and therefore, their combination formed a hybrid reinforcement consisting of cellulosic materials from different length scales and with different morphology.

Experimental methods

Preparation of aqueous MCC suspensions

Aqueous suspensions of MCC were prepared for dispersion study as well as for fabricating cementitious composites. To prepare the suspensions, weighed amount of MCC powder was added to 20 mL of distilled water. The amounts of MCC added to water were 0.1%, 0.2%, 0,4%, 0.6%, 0.8%, 1%, 1.2%, 1.5%, 1.6%, 2.0% and 3.0% MCC (by weight of water). Then, MCC was mixed properly with water with the help of magnetic stirring and soaked for 2 days. Following that, CTAB was added to the suspensions through magnetic stirring for 10 min. The amounts of CTAB added to the suspensions were 20%, 40% and 60% of MCC weight. MCC suspensions were then sonicated in a bath ultrasonicator (Sonica® Ultrasonic Clear) for 15 min. The suspensions for developing cementitious composites were prepared using the above process but with the optimized amount of CTAB along with the defoaming agent, TBP. To compare the dispersion ability of CTAB with that of previously used Pluronic F-127 surfactant (Parveen

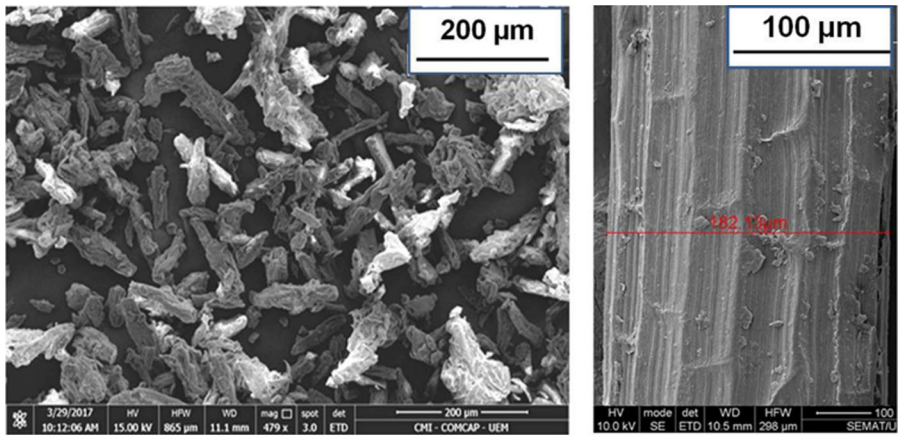

Fig. 1 Morphology of MCC (**a**) and sisal fibers as characterized through SEM (**b**)

et al. 2017b), aqueous suspensions with different MCC concentrations were also prepared using 20% Pluronic F-127 (of MCC weight) using the same process.

Characterization of quality of MCC suspensions

Optical microscopy The aqueous suspensions of MCC and MCC containing CTAB were characterized for dispersion homogeneity, sedimentation and agglomeration by observing visually and through optical microscopy (Olympus BH-2) after 48 h of their preparation. The optical microscopy was performed using a drop of MCC suspension taken on a glass slide and observing at different locations of suspensions under different magnifications. The overall homogeneity or MCC distribution in the suspensions and the presence of individually dispersed and agglomerated MCC were observed and compared for different suspensions.

UV–Vis spectroscopy Aqueous suspensions containing different concentrations of MCC and MCC with CTAB were characterized by UV–Vis spectroscopy (UV-2401PC, UV–VIS Recording Spectrophotometer, Shimadzu) to measure absorption intensity (after 48 h of preparation). The concentration of only well dispersed MCC was characterized by UV–Vis spectroscopy as agglomerated MCC settled down at the bottom of the suspensions. The absorption intensity at 300 nm was compared for different suspensions to find out the optimum MCC and CTAB concentrations.

Fabrication of plain and hierarchical cementitious composites

The fabrication of plain mortar samples was carried out by mixing OPC (450 g), standardized sand (1350 g) and distilled water (225 mL) in the proportion of 1:3:0.5 using a Hobart mixer according to NP EN 196-1:2006 standard. Hierarchical cementitious composites were prepared by adding MCC aqueous suspensions (225 mL, containing 40% CTAB and TBP) and sisal fibers to the cement and standardized sand mixture. The amounts of MCC added to the cement mixture were 0.1%, 0.2%, 0.4%, 0.6%, 0.8%, 1.0% and 1.5% on the weight of cement. The amounts of sisal fibers were 0.25% and 0.50% of cement weight. The MCC aqueous suspensions were immediately used after their preparation to avoid MCC sedimentation. CTAB produced foam in the cement mixture and therefore, TBP was used to suppress foam formation. In order to find out the optimum ratio of TBP, cementitious composites were fabricated with 0%, 50%, 75% and 100% TBP (on the weight of CTAB). After proper mixing, the prepared mortar paste was poured into standard rectangular molds with dimensions of 160 mm × 40 mm × 40 mm and kept in a humid chamber according to NP EN 196-1:2006 standard. After 24 h, the samples were demolded and kept under water for 28 days to carry out hydration. After 28 days, the samples were taken out from water, wiped out and then tested for flexural and compressive properties. Another set of samples containing only MCC (0.1 wt% and 1.0 wt%) and only sisal fibers

(0.25 wt% and 0.50 wt%) were prepared for the comparison purpose using the same procedure but without using CTAB and TBP.

Characterization of processability of mortar paste

The flow behavior of plain mortar paste and pastes of hierarchical composites were measured using a flow table disc according to EN 1015-3:2004 standard. This test was performed to analyze the influence of MCC, sisal fibers and surfactant on the flow behavior of mortar paste. The flow behavior was characterized from the diameters of mortar paste measured in both horizontal and vertical directions on a flow table disc after standardized vertical impacts. A larger paste diameter indicated superior flow properties and processability of mortar. The average of the horizontal and vertical diameters has been calculated and presented in this paper.

Characterization of mechanical performance

Flexural and compressive strength Plain mortar and hierarchical cementitious composites were characterized for flexural and compressive properties according to NP EN 196-1:2006 standard. The fracture energy in the flexural mode was calculated from the area under the load-elongation curves using Origin software. For flexural testing, 3 prism shaped specimens with 160 mm × 40 mm × 40 mm dimension from each composite category were tested at 50 N/s speed using a preload of 50 N. The compression test was performed on the two halves of the ruptured specimens from the flexural test, i.e., on 80 mm × 40 mm × 40 mm samples at a 500 N/s testing speed.

Fiber-matrix interfacial bonding Single fiber pull-out test was performed to determine adhesion of sisal fibers to the cementitious matrix in both plain mortar and hierarchical composites. A single sisal fiber (20 cm) was inserted (at 2 cm depth) in a cylindrical shaped mold (2.54 cm diameter) containing plain mortar or hierarchical composite pastes. The cylindrical samples were hydrated for 7 and 28 days. Ten samples were prepared for each type of composites. After curing, the specimens were tested in a dynamometer (Hounsfield H10 KS) with a 2500 N load cell and at a speed of 2 mm/min. Force was applied to the sisal fiber until it was completely removed from the matrix or ruptured, and the force–displacement curve was recorded.

Fracture behavior through digital image correlation The fracture and crack propagation in cementitious composites were studied using digital image correlation (DIC) technique. Tests were performed on plain mortar and hierarchical composites containing 0.5% sisal with and without 0.1% MCC (160 mm × 40 mm × 40 mm). After hydration, a notch of 6 mm was introduced into the samples according to Single Edge Notched Bend (SENB) configuration. The surface of the specimens was painted with a white synthetic paint and next, a black paint was sprayed. This contrast allowed to study the samples using DIC, comparing the images taken in every 2 s. The fracture behavior and crack propagation were studied in the flexural mode. Loads and crack mouth opening displacement (CMOD) were recorded using linear variable differential transducers and the images were processed using the GOM Correlate software.

Characterization of microstructure of cementitious composites

Characterization of density and pore structure The density of plain mortar and selected hierarchical cementitious were measured using Pycnometry by intrusion of Helium gas. The analysis was carried out on Micromeritics equipment (model: AccuPyc II 1340) in cycles of three determinations per aliquot. The samples were taken from the composites after fracturing in mechanical tests (flexural and compressive). Then the samples were stored in hermetically sealed plastic containers kept in the laboratory at room temperature. Prior to the testing, the samples were dried at 60 °C for 24 h and kept in a desiccator. The samples were broken into a size of approximately 1 cm^3 for the measurement. Pore size distribution and porosity of plain mortar and selected hierarchical cementitious composites (0.1% MCC + 0.5% sisal) were analyzed using mercury intrusion porosimetry (MIP) in Micromeritics AutoPore IV 9500 V1.07 instrument, according to BS ISO 15901-1:2005 standard. In MIP, the pore size distribution was determined by forcing mercury into a sample (1 cm^3) under increasing pressure and

measuring the volume of mercury intruded as a function of pressure. A pressure range of 0.0007 to 414 MPa was used to allow measurement of pore size ranging from 340 μm to 5 nm. An advancing/receding contact angle of mercury of 130° and surface tension of 0.485 N/m were used.

Characterization of hydration products through DTG and XRD analyses Hydrated specimens (after mechanics tests) were stored in hermetically sealed plastic containers (to avoid carbonation) kept in the laboratory at room temperature for thermogravimetric analysis (TGA). Prior to the analysis, specimens were dried at 60 °C for 48 h and then crushed to make a powder. Plain mortar and selected hierarchical cementitious composites were characterized by TGA (Hitachi STA 7200) in a nitrogen atmosphere at a heating rate of 10 °C/min up to a temperature of 900 °C. The quantitative estimation of different hydration products such as C-S–H, $Ca(OH)_2$, $CaCO_3$, etc. was performed using derivative thermogravimetry (DTG) curves of the specimens. The influence of MCC on the hydration degree of cement was studied from this characterization. Plain mortar and selected hierarchical cementitious composites were characterized using X-ray diffraction (XRD) to investigate various hydration products. XRD analysis was carried out using Bruker D8 Discover diffractometer in the angle range of 5°–70° with step size of 0.04 and 2 s per step.

Characterization of durability of cementitious composites

Measurement of water absorption Water absorption due to capillary action in hardened mortar and cementitious composites was characterized according to BS EN 1015-18: 2002 standard. Samples with 160 mm × 40 mm × 40 mm size were sealed with silicone on four long faces and ruptured in flexure in two halves. Subsequently, the samples were oven dried at 60 ± 5 °C until a constant weight was obtained. The samples were then immersed in water at a depth of 5 to 10 mm in a suitable container (plastic box with a wide flat area). This test was performed over a total period of 30 days on plain mortar and composite samples containing 0.1% MCC and 0.5% sisal fibers (both on the weight of cement). The coefficient of water absorption was calculated from the slope of the straight line connecting the representative points of measurements made at 10 min and 90 min of immersion, according to the following formula:

$$C = 0.1 * \frac{(m2 - m1)}{A * t^{0.5}} \quad (1)$$

where m1 is the sample mass after 10 min immersion in gm, m2 is the sample mass after 90 min immersion in gm, A is the cross-sectional area of the specimen in contact with water, t is the time in min.

Measurement of carbonation resistance The determination of carbonation resistance of plain mortar and cementitious composites at accelerated conditions was performed according to EN 12390-12: 2010 standard. The prism shaped samples were conditioned in a laboratory environment for 14 days prior to sealing the top, bottom and two opposite side faces of the specimens. After sealing of all but two faces, the samples were placed in a storage chamber with a carbon dioxide level of 4.0 ± 0.5%, temperature of 20 ± 2 °C and relative humidity of 55 ± 5% for a period of at least 70 days. After each exposure period (2, 4, 9, 14, 21, 28, 56 and 70 days), a 50 mm slice was broken from each sample and observed for carbonation depth. After splitting off a slice, the split end faces of the samples were sealed and the sample was then returned to the storage chamber.

Accelerated ageing test The durability of plain mortar and hierarchical cementitious composite samples (with 0.1% MCC + 0.5% sisal) was evaluated by subjecting them to accelerated aging cycles in a climatic chamber (Fitoclima 1000EC45) at a temperature range of −10 °C to +30 °C and a relative humidity up to 90%. The samples were tested after 28 days of water cure and subsequent 14 days cure at room temperature and tested for 9 cycles, 18 cycles, 27 cycles and 90 cycles corresponding to 6, 12, 18 and 60 days in the climate chamber. After the period of exposure, the samples were oven dried at 60 °C and characterized for compressive strength. Sisal fibers removed from the samples were characterized by scanning electron microscopy (SEM) and Fourier transform infrared spectroscopy (FTIR) to observe change in their morphology and chemical structure.

Results and discussion

Dispersion state of microcrystalline cellulose

MCC aqueous suspensions prepared without CTAB and with 20%, 40% and 60% of CTAB, after 15 min of ultrasonication are shown in Fig. 2. MCC concentration in these suspensions was varied from 1 to 3 wt%. CTAB is a ionic surfactant possessing a cationic head group which can interact with the anionic surface of MCC particles, which are then stabilized due to the ionic and steric repulsions between the surfactant molecules (Eyley and Thielemans 2014), as schematically presented in Fig. 3. The N^+ cations of CTAB molecules get attracted by the Cl^- anions on the MCC surface (generated during Avicel® PH-101 MCC synthesis due to acid hydrolysis by HCl, as per the manufacturer's information) and the stabilization of MCC occurs due to ionic (due to positive charge) and steric repulsions (due to long aliphatic tails) between CTAB molecules. From Fig. 2b, it can be clearly observed that MCC suspensions with 40% CTAB had a better MCC dispersion (the suspensions appeared to be more white) as compared to suspensions without CTAB as well as with 20% and 60% of CTAB. The later suspensions appeared to be more transparent due to lower amount of dispersed MCC and more sedimentation at the bottom of the vials. Previous studies also indicated a better MCC dispersion at an optimum concentration (20%) of Pluronic F-127 surfactant and at higher or lower Pluronic concentrations, the stability of the suspensions deteriorated (Parveen et al. 2017b). This could be attributed to the fact that at high concentrations CTAB molecules could form considerable amount of micelles resulting in sedimentation of MCC particles. This was previously evidenced in case of CNT dispersion with CTAB above critical micellar concentrations (Rastogi et al. 2008; Clark et al. 2011). This observation has

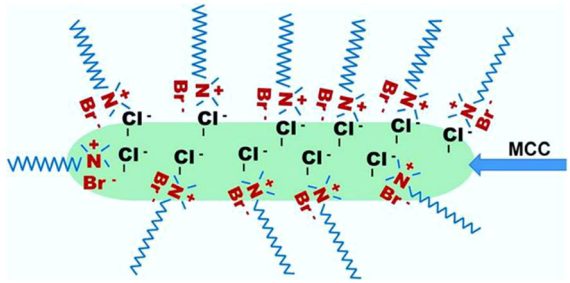

Fig. 3 Schematic of MCC stabilization by CTAB molecules

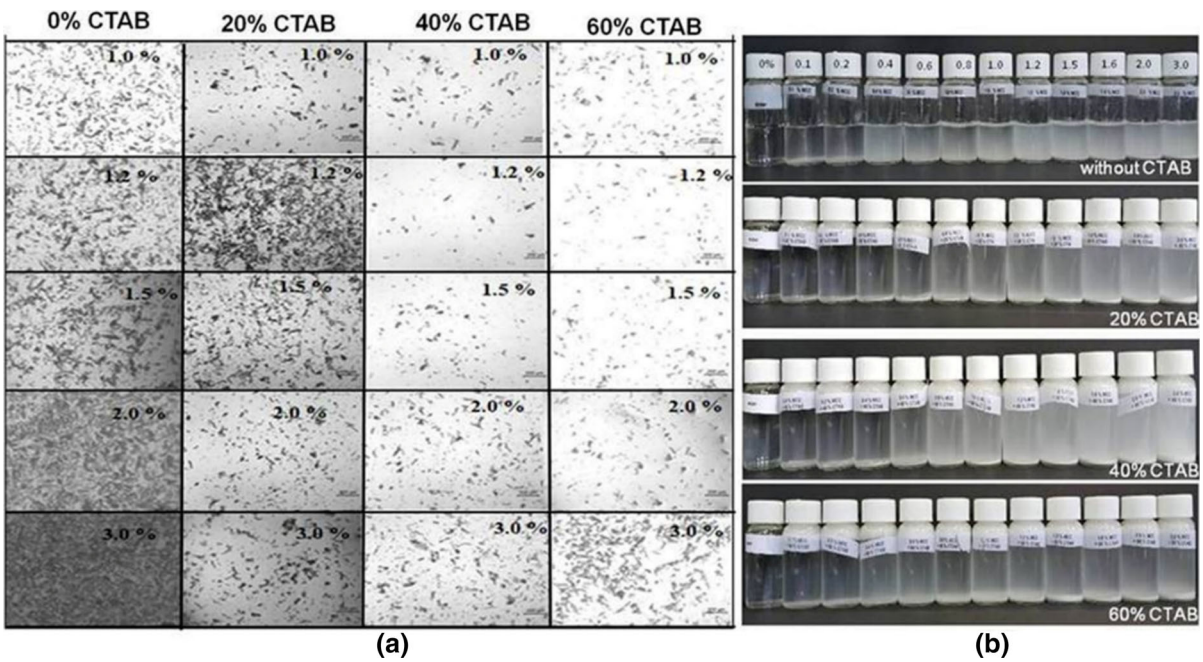

Fig. 2 1–3 wt% MCC suspensions prepared without and with 20%, 40% and 60% CTAB observed through optical microscopy (**a**) and visually (**b**)

been confirmed from the optical micrographs presented in Fig. 2a. It is clear that the MCC dispersion was more homogeneous at 40% CTAB concentration as compared to the 20% and 60% CTAB-based suspensions, which showed significant MCC agglomeration.

The agglomerated area calculated from optical micrographs is presented in Fig. 4. It supports the qualitative observation, i.e. the highest agglomerated area was noticed in suspensions prepared without surfactant and the lowest value was achieved with 40% CTAB. It can also be noticed from both optical micrographs and agglomerated area that the increase in MCC concentration increased MCC agglomeration at all CTAB concentrations, which was also previously noticed in case MCC suspensions prepared with or without surfactants (Parveen et al. 2017b, 2018). The MCC agglomerated area obtained with CTAB in the present study was significantly lower as compared to suspensions prepared with only ultrasonication (Parveen et al. 2017a) (which resulted in ∼ 16% agglomerates using 30 min ultrasonication as compared to only ∼ 5% agglomerates using CTAB and 15 min ultrasonication) due to the positive role of CTAB in MCC dispersion. Also, it is clear from Fig. 4 that the agglomerated area was significantly lower in all CTAB concentrations (and much lower with 40% CTAB) as compared to the Pluronic F-127 based suspensions, indicating better MCC dispersion ability of CTAB as compared to Pluronic F-127. This could be due to the fact that Pluronic F-127 can stabilize MCC particles only through steric stabilization (Parveen et al. 2017b), whereas both steric and ionic repulsion mechanisms are possible with CTAB. The UV–Vis absorbance of suspensions containing different MCC concentrations (0–3 wt%) at 300 nm is presented in Fig. 5 (see Fig. 15, Appendix for UV–Vis spectra). It is notable that absorbance increased with MCC concentrations; the increase was linear at low MCC concentrations confirming that MCC added to the suspensions remained in the dispersed phase. However, deviation of the curves from a linear shape at higher concentrations indicated that some amount of added MCC resulted in agglomeration and sedimentation at higher MCC concentrations, as also observed earlier in case of CNT suspensions (Rastogi et al. 2008). It can be clearly observed that the absorbance of suspensions with 40% CTAB concentration was significantly higher indicating higher quantity of dispersed particles and better dispersion quality as compared to the other concentrations. This finding supports the observations made in visual observation and optical microscopy presented in Figs. 2 and 4. It can also be observed that 20% Pluronic F-127 based suspensions showed lower absorbance as compared to 40% CTAB based suspensions, indicating a superior stability of MCC suspensions with 40% CTAB as compared to 20% Pluronic F-127. Based on these experimental observations, 40% CTAB was selected as the optimum surfactant concentration for dispersing MCC and subsequently fabricating cementitious composites.

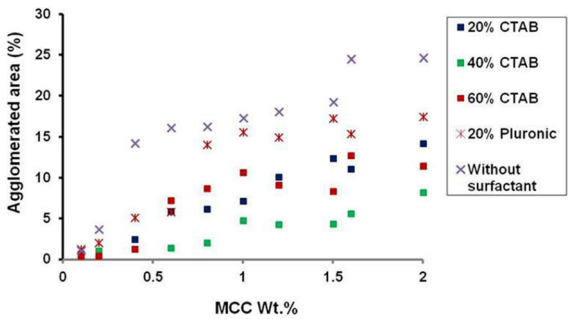

Fig. 4 Agglomerated area of MCC in different suspensions prepared without and with CTAB

Quality of freshly prepared mortar pastes

The consistence, which represents the flow properties or workability of fresh pastes of plain mortar and

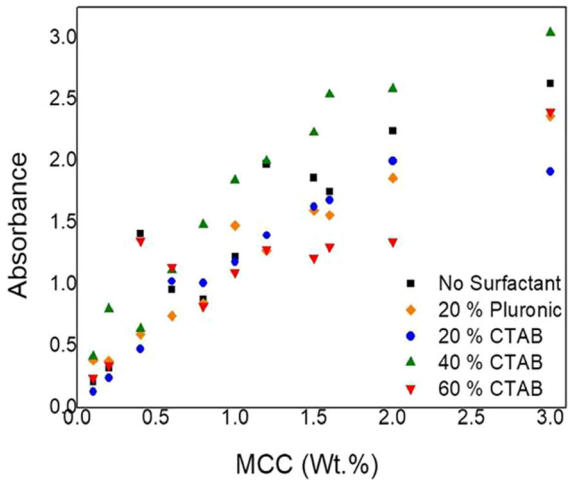

Fig. 5 Absorbance of MCC suspensions (at 300 nm) at different concentrations (0–3 wt%)

hierarchical composites, is presented in Fig. 6a from which the influence of MCC and sisal fiber content on the consistence can be observed. An increase in sisal fiber content from 0.25 to 0.5 wt% reduced the flow behavior of composites up to 0.4 wt% MCC (which was mainly due to water absorption by sisal fibers), after which it became similar. At the same sisal fiber content, flow properties of fresh mortar first decreased up to 0.2% MCC and then increased until 0.8% MCC, after which it started to decrease again. The initial decrease in consistence was attributed to the water retention by hydrophilic MCC (similar to sisal fibers), reducing flow properties of the mortar paste. At higher MCC %, the increased amount of surfactant used could improve the flow properties by ensuring proper dispersion of both cement and MCC particles. It was also noticed in the previous studies that an excessive use of surfactant resulted in considerable increase in the consistence of mortar paste (Parveen et al. 2015). At a MCC concentration higher than 0.8% (i.e., 1.6% in aqueous suspension), a considerable increase in MCC agglomeration (as shown in Fig. 2) resulted in further decrease in the flow properties. It is also evident from Fig. 6a that the flow properties of mortar paste was more influenced by MCC at higher concentrations as compared to sisal fiber (in the studied range) mainly due to higher surface area of MCC that led to rapid water absorption or severe agglomeration, affecting flow properties considerably.

Although the use of CTAB proved helpful in maintaining flow properties of mortar paste, it led to significant production of air pockets in the mortar paste, as previously reported in case of other surfactants (Parveen et al. 2015, 2017b). An optimized quantity of defoamer was extremely important to suppress the produced foam (Parveen et al. 2015). If the generation of foam was not suppressed, its presence could lead to increase in porosity of hydrated mortar and deterioration of mechanical properties (Parveen et al. 2015). The influence of defoamer in reducing pores can be seen in Fig. 6b. Pores on the surface of hydrated samples can be clearly observed in case of 0%, 50% and 75% TBP, while an increase in the TBP % showed gradual reduction in the surface porosity. The sample prepared with 100% TBP exhibited very low surface porosity indicating effective suppression of foam by the defoamer. Previous research on MCC-CNT reinforced cementitious composites also suggested 1:1 as the optimum TBP: CTAB ratio for preparing cementitious composites with low porosity and good mechanical properties (Alshaghel et al. 2018). In case of Pluronic F-127 surfactant, a 0.5:1 ratio of TBP: Pluronic was found sufficient in suppressing foam formation and prepare composites with low volume of pores (Alshaghel et al. 2018).

Mechanical properties of cementitious composites

Compressive and flexural strengths

The compressive and flexural strengths of plain mortar, mortar with only MCC (0.1 wt% and 1.0 wt%) and only sisal fibers (0.25 wt% and 0.5 wt%) and hierarchical cementitious composites developed using

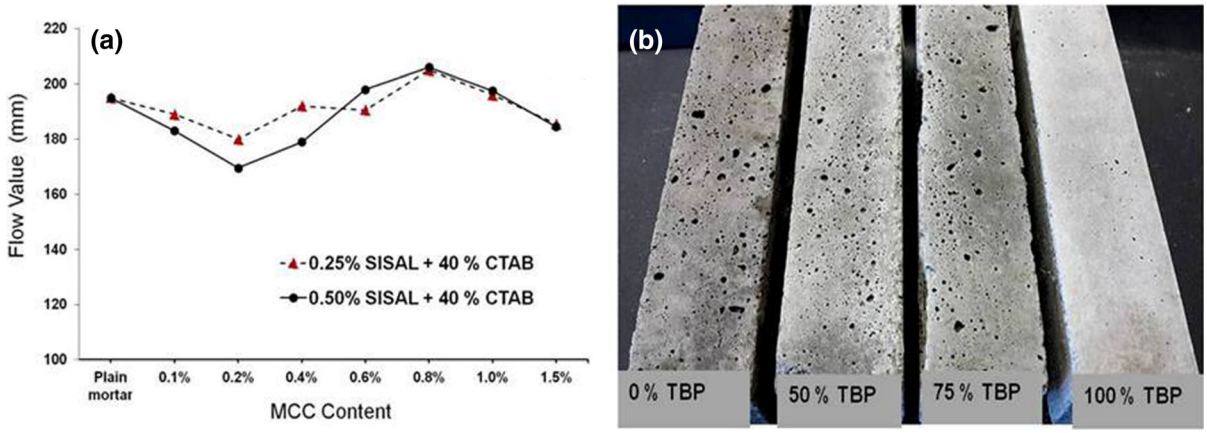

Fig. 6 **a** Influence of MCC and sisal fiber on the flow values of fresh mortar paste and **b** influence of defoamer content on the quality of cementitious composites

MCC (0.1 to 1.5 wt%), sisal fibers (0.25 wt% and 0.50 wt%) and 40% CTAB are listed in Table 2. It can be noticed that the use of only MCC (0.1 wt% and 1.0 wt%) improved the compressive strength significantly (by ~ 21% and 17%, respectively), but deteriorated the flexural strength. The negative effect of MCC on the flexural strength (which was more affected by voids and defects present in the composites than the compressive strength) was attributed to the MCC agglomerates which formed in the suspensions when prepared without CTAB (see Fig. 2). The short ultrasonic treatment for 15 min used in this research could not effectively remove the MCC agglomerates without using CTAB surfactant. Previous studies which showed a positive effect of MCC on the flexural strength of cementitious composites either used longer durations of ultrasonication/mechanical stirring or used surfactants (Parveen et al. 2017b, 2018; Silva et al. 2018). It can also be noticed that the use of only sisal fibers (0.25 wt% and 0.5 wt%) led to decrease in both compressive and flexural strengths, as also reported in the existing literature. However, the influence of hybrid reinforcement on compressive strength of mortar was quite positive and promising. Compressive strength improved significantly at lower MCC concentrations (e.g. 0.1 wt% MCC). 0.1% MCC along with 0.25% and 0.5% sisal fibers improved compressive strength by ~ 23% and ~ 24%, respectively. Sisal fiber content, therefore, did not show any significant positive influence on compressive strength, as previously reported in other studies also (Fujiyama et al. 2014). However, an increase in MCC % drastically reduced the compressive strength owing to MCC agglomeration (Parveen et al. 2017b, 2018; Alshaghel et al. 2018; Silva et al. 2018), irrespective of the sisal fiber content. A similar trend was also observed in case of flexural strength, which was found to be inferior at higher MCC concentrations (> 1 wt%). However, in contrast to compressive strength, an increase in sisal fiber content from 0.25 wt% to 0.5 wt% led to significant improvement in flexural strength. The highest improvement in flexural strength of ~ 18% was achieved with 0.1% MCC and 0.5 wt% sisal fibers. The positive effect of sisal fibers on flexural strength in the hierarchical composites could be due to crack-bridging ability of sisal fibers

Table 2 Compressive strength of plain cement mortar and hierarchical cementitious composites

Samples	Compressive strength (MPa)	Increase (%)	Flexural strength (MPa)	Increase (%)
Plain mortar	42.3 ± 0.8	–	6.6 ± 0.1	–
0.1% MCC	51.0 ± 0.9	20.6	6.5 ± 0.1	− 1.5
1% MCC	49.5 ± 0.7	17.0	6.1 ± 0.2	− 7.6
0.25% sisal	40.8 ± 1.4	− 3.5	6.3 ± 0.7	− 4.5
0.5% sisal	39.4 ± 0.8	− 6.9	6.1 ± 0.5	− 7.5
0.1% MCC + 0.25% sisal	51.9 ± 1.6	**22.6**	6.8 ± 0.1	**2.2**
0.2% MCC + 0.25% sisal	40.3 ± 3.6	− 4.8	5.9 ± 0.2	− 11.9
0.4% MCC + 0.25% sisal	34.7 ± 3.3	− 18.1	5.2 ± 0.2	− 22.3
0.6% MCC + 0.25% sisal	33.7 ± 1.6	− 20.5	5.9 ± 0.7	− 10.8
0.8% MCC + 0.25% sisal	11.9 ± 1.5	− 71.8	3.1 ± 0.1	− 53.4
1.0% MCC + 0.25% sisal	41.2 ± 0.9	− 2.55	6.5 ± 0.1	− 2.3
1.5% MCC + 0.25% sisal	40.4 ± 3.7	− 4.6	6.5 ± 1.0	− 2.7
0.1% MCC + 0.50% sisal	52.5 ± 0.9	**24.2**	7.8 ± 0.4	**18.2**
0.2% MCC + 0.50% sisal	38.1 ± 3.1	− 9.9	7.0 ± 0.3	**4.7**
0.4% MCC + 0.50% sisal	32.9 ± 2.1	− 22.3	5.7 ± 0.6	− 14.9
0.6% MCC + 0.50% sisal	36.6 ± 2.5	− 13.6	6.6 ± 0.2	− 1.1
0.8% MCC + 0.50% sisal	42.7 ± 4.7	**1.0**	6.4 ± 1.1	− 3.5
1.0% MCC + 0.50% sisal	41.8 ± 1.2	− 1.1	6.1 ± 0.3	− 7.9
1.5% MCC + 0.50% sisal	39.5 ± 1.6	− 6.8	6.0 ± 0.2	− 8.9

The values in bold represent the positive values, i.e. increase in the compressive and flexural strengths

(Savastano et al. 2009; Silva et al. 2009; Fujiyama et al. 2014), which prevented a faster crack growth and brittle failure of composites.

This can be confirmed from the flexural strain and fracture energy data, listed in Table 3. The improvements in compressive and flexural strengths were lower in the developed hierarchical composites as compared to MCC reinforced cementitious composites fabricated using ultrasonication and surfactants (Parveen et al. 2017b, 2018). Previously reported CNT-MCC hierarchical composites also showed lower improvement in compressive and flexural strengths as compared to MCC or CNT reinforced cementitious composites, but superior fracture energy and ductility (Alshaghel et al. 2018), as similar to the hierarchical composites investigated in the present study. While inferior dispersion of MCC-CNT hybrid reinforcement as compared to the individual components (i.e., MCC or CNT) was the main reason behind lower strength of these hierarchical composites (Alshaghel et al. 2018), the lower strength of the studied hierarchical composites was attributed to the negative influence of sisal fibers on composite's microstructure and strength.

It can be observed from Table 3 that the use of only MCC significantly reduced both flexural strain and fracture energy of mortars. In case of hierarchical composites, the flexural strain was significantly higher than plain mortar at 0.1% MCC (at both 0.25% and 0.5% sisal fibers) and an increased MCC content drastically reduced the flexural strain below the plain mortar values, in most of the cases. The decreased flexural strain due to MCC addition was observed earlier in both cementitious and polymeric composites and was attributed to the stiffening effect of MCC due to its crystalline structure (Liu et al. 2017). The use of only sisal fibers in mortars also showed negative effects on both flexural strain and fracture energy; however, the fracture energy was higher at the higher sisal fiber content (although lower than plain mortar values). The increase in sisal fiber content, in the hierarchical composites, showed a positive influence on the flexural strain of composites, increasing by $\sim$ 28% at 0.5% sisal fibers. A similar trend was also noticed in case of fracture energy (at flexural mode), which exhibited an increase of 40% over plain mortar values with 0.1% MCC and 0.5% sisal fibers. The increase in the flexural strain and fracture energy of hierarchical composites due to sisal fibers was mainly attributed to the crack bridging ability of sisal fibers (Onésippe et al. 2010; Fu et al. 2017). It was interesting to note that the incorporation of sisal fibers

Table 3 Flexural strain and fracture energy of plain mortar and hierarchical composites

Samples	Strain (%)	Increase (%)	Fracture energy (J)	% Increase
Plain mortar	0.0057 ± 0.0002	–	0.27 ± 0.02	–
0.1% MCC	0.0056 ± 0.0002	− 1.7	0.16 ± 0.02	− 40.7
1% MCC	0.0052 ± 0.0003	− 8.8	0.16 ± 0.03	− 40.7
0.25% sisal	0.0055 ± 0.0004	− 3.5	0.23 ± 0.02	− 14.8
0.5% sisal	0.0053 ± 0.0006	− 7.0	0.26 ± 0.04	− 3.7
0.1% MCC + 0.25% Sisal	0.0066 ± 0.0017	**15.8**	0.22 ± 0.05	− 15.4
0.2% MCC + 0.25% Sisal	0.0035 ± 0.0003	− 38.5	0.18 ± 0.02	− 32.7
0.4% MCC + 0.25% Sisal	0.0035 ± 0.0002	− 38.5	0.16 ± 0.01	− 40.6
0.6% MCC + 0.25% Sisal	0.0041 ± 0.0004	− 28.1	0.21 ± 0.04	− 22.9
0.8% MCC + 0.25% Sisal	0.0036 ± 0.0003	− 36.5	0.09 ± 0.01	− 67.7
1.0% MCC + 0.25% Sisal	0.0054 ± 0.0003	− 5.8	0.26 ± 0.01	− 1.1
1.5% MCC + 0.25% Sisal	0.0058 ± 0.0004	**2.2**	0.27 ± 0.06	**2.9**
0.1% MCC + 0.50% Sisal	0.0073 ± 0.0005	**27.8**	0.37 ± 0.04	**40.3**
0.2% MCC + 0.50% Sisal	0.0057 ± 0.0003	–	0.29 ± 0.01	**8.2**
0.4% MCC + 0.50% Sisal	0.0046 ± 0.0004	− 18.7	0.22 ± 0.04	− 16.0
0.6% MCC + 0.50% Sisal	0.0071 ± 0.0010	**24.8**	0.29 ± 0.02	**10.1**
0.8% MCC + 0.50% Sisal	0.0060 ± 0.0004	**5.8**	0.28 ± 0.06	**5.1**
1.0% MCC + 0.50% Sisal	0.0052 ± 0.0004	− 8.9	0.23 ± 0.02	− 11.7
1.5% MCC + 0.50% Sisal	0.0048 ± 0.0003	− 15.9	0.23 ± 0.02	− 14.6

The values in bold represent the positive values, i.e. increase in the strain and fracture energy

resulted in a post-peak load-carrying capability and prevented sudden failure of composites (as shown in Fig. 16, Appendix). This type of post-cracking load-carrying ability was also noticed earlier in case of carbon nanofiber (CNF)-polyvinyl alcohol (PVA) microfiber and CNF-steel fiber reinforced hierarchical cementitious composites, in which PVA microfibers and steel fibers mainly improved the post-cracking behavior of composites (Metaxa et al. 2010; Alrekabi et al. 2017). Therefore, the findings of the mechanical characterisation suggests that the combination of MCC and sisal fibers worked much better than the individual components showing a synergistic effect and as a result, the hybrid reinforcement was able to significantly improve both strength and fracture energy of mortars. In hierarchical composites, the compressive strength was mainly improved by MCC, whereas sisal fibers improved the flexural strength and fracture energy.

Fracture behavior and interfacial bonding

The crack propagation behavior of plain mortar and hierarchical the composites containing 0.1% MCC and 0.5% sisal fibers is shown in Figs. 7 and 8. It can be noticed that a single macro-crack was formed in these samples above the notch. The time for the fracture initiation, to reach peak load and the end of the test is listed in Table 4. It is clear that fracture initiated quickly in the plain mortar sample, which also reached the peak load and complete fracture (no load-bearing) much quicker as compared to the samples containing 0.5% sisal fibers and hierarchical composites. Moreover, as compared to sisal fiber composites, hierarchical composites showed a delayed fracture initiation and reached peak load earlier although continued to bear the load for a longer period of time. The longer fracture initiation and completion times in case of hierarchical composites as compared to sisal fiber composites clearly suggests a synergistic effect of the hybrid reinforcement on the fracture behavior and is expected to result due to effective load-sharing between MCC and sisal fibers controlling the fracture of composites. This was also supported by the fracture energy values, which increased by 40% in case of hierarchical composites, as discussed earlier. This behavior, which is often called a pseudo-ductile behavior where hybridization of reinforcing materials results in higher strain and fracture energy of composites, was previously noticed mainly in case of polymeric composites (Swolfs et al. 2014).

Improved ductile behavior of hierarchical cementitious composites as resulted from the crack-bridging of sisal fibers required good interfacial bonding between sisal fibers and cementitious matrix to avoid complete fiber pull-out from the matrix. However, untreated sisal fibers were found to present an inferior interface with cementitious composites (Lima et al. 2017).

It is very interesting to note in the present study that the use of MCC significantly improved the sisal fiber-cementitious matrix bonding as shown in Fig. 9. The samples used for pull-out testing and the test setup are shown in Fig. 9b, c. The pull-out force of sisal fibers from the cementitious matrix improved by 54% and 51% using 0.1% MCC at 7 and 28 hydration periods, respectively. The fracture surface (after flexural testing), as shown in Fig. 9d, also showed good fiber-matrix bonding leading to partial fiber pull-out during fracture of composites. Previous studies demonstrated that nanocellulose could improve the hydration behavior of cement at the plant fiber surface and improved the fiber-matrix bonding (Mohammadkazemi et al. 2015). As MCC particles were homogeneously dispersed in the matrix, MCC particles that were present in the interfacial region improved cement hydration and consequently, the bonding between the fibers and the matrix. Another possible reason behind improved interfacial strength could be the formation of hydrogen bonds between the hydroxyl groups of sisal fibers and MCC particles, as previously observed in case of MCC reinforced hierarchical polymeric composites (Pichandi et al. 2018).

Hydration behavior of plain mortar and cementitious composites

The derivative weight loss (DTG) curves of plain mortar and selected hierarchical cementitious composites are shown in Fig. 10a. The DTG curves showed four major peaks due to hydration reactions occurred during setting of cementitious composites. As reported by previous researchers, the first peak (40–60 °C) was due the evaporation of water from calcium silicate hydrate (C-S–H) phase, the second peak (110–145 °C) was due to evaporation of water from ettringite, the third peak ($\sim$ 400 °C) was due to the decomposition of calcium hydroxide $Ca(OH)_2$ and

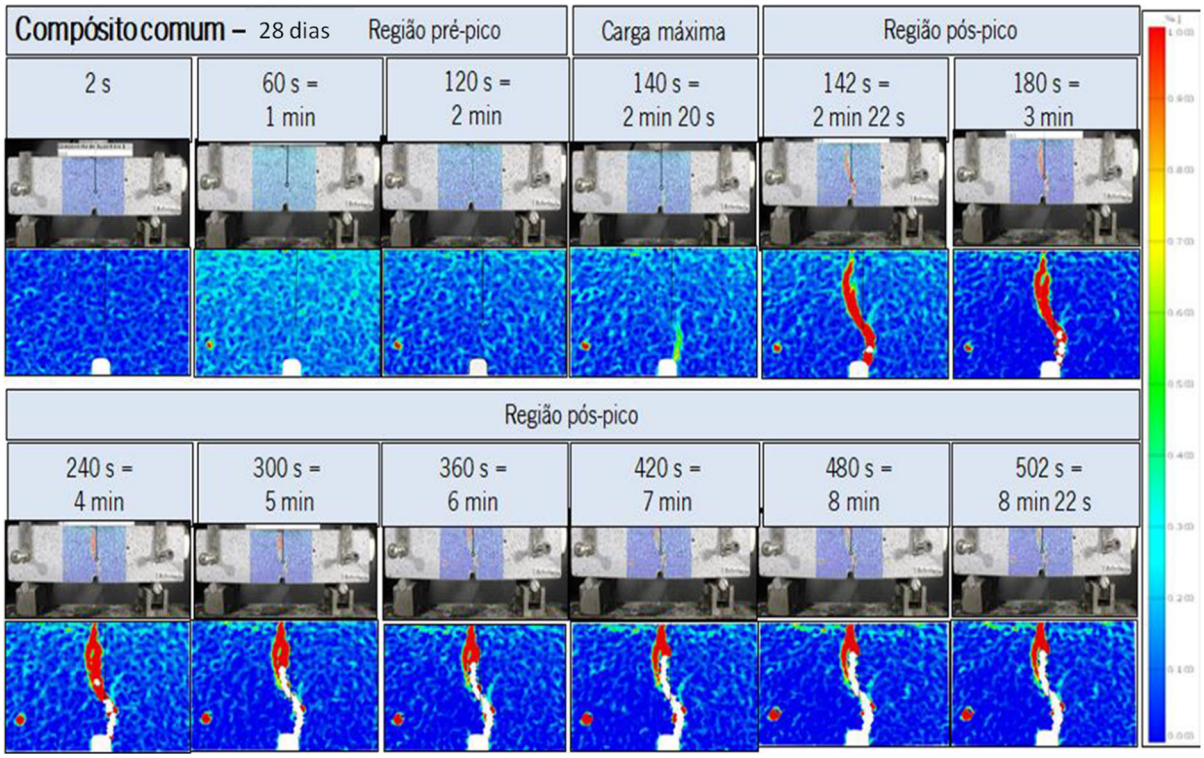

Fig. 7 Crack propagation behavior of plain mortar as studied by DIC method

the fourth peak (~ 650 °C) represented the calcium carbonate decomposition (Parveen et al. 2017b). Enlarged views of these peaks for selected composites are shown in Fig. 10b.

It can be observed that the intensity of C–S–H and $Ca(OH)_2$ peaks increased strongly in case of hierarchical composites as compared to plain mortar. This clearly indicates formation of higher amount of hydration products in case of hierarchical composites. Moreover, the highest peak intensities were obtained in case of hierarchical composites containing 0.1% MCC indicating superior hydration in these hierarchical composites. The reason behind better hydration in hierarchical composites could be the short circuit diffusion (SCD) of water through MCC as proposed earlier by Cao et al. for nanocellulose (Cao et al. 2015). Moreover, MCC could contribute to better cement hydration by controlling release of water, i.e. retaining water in the initial phase and slowly releasing it as the hydration continued (Parveen et al. 2017b). Homogeneous (almost individual particle) dispersion in case of 0.1% MCC resulted in higher MCC surface area, which contributed to superior SCD and water adsorption in the initial hydration phase and resulted in better hydration. The peak of $Ca(OH)_2$ of hierarchical composites at different hydration periods, as shown in Fig. 10c, also indicated that the amount of $Ca(OH)_2$ increased as the hydration period increased from 4 h to 56 days. In Fig. 10b, it can be clearly observed that plain mortar showed the highest peak of $CaCO_3$ among all other cementitious composites. The hierarchical composites suppressed the formation of $CaCO_3$ due to less penetration of atmospheric CO_2 to react with $Ca(OH)_2$. This occurred due to a denser microstructure resulting from better hydration products. Previous studies also reported lower $CaCO_3$ formation in case of CNT, MCC, and MCC-CNT hierarchical cementitious composites (Parveen et al. 2015, 2017b; Alshaghel et al. 2018). This finding was further supported by the porosity measurements as discussed in "Degradation of cementitious composites" section. The lowest formation of $CaCO_3$ in case of 0.1% MCC containing hierarchical composites could be attributed to better MCC dispersion that

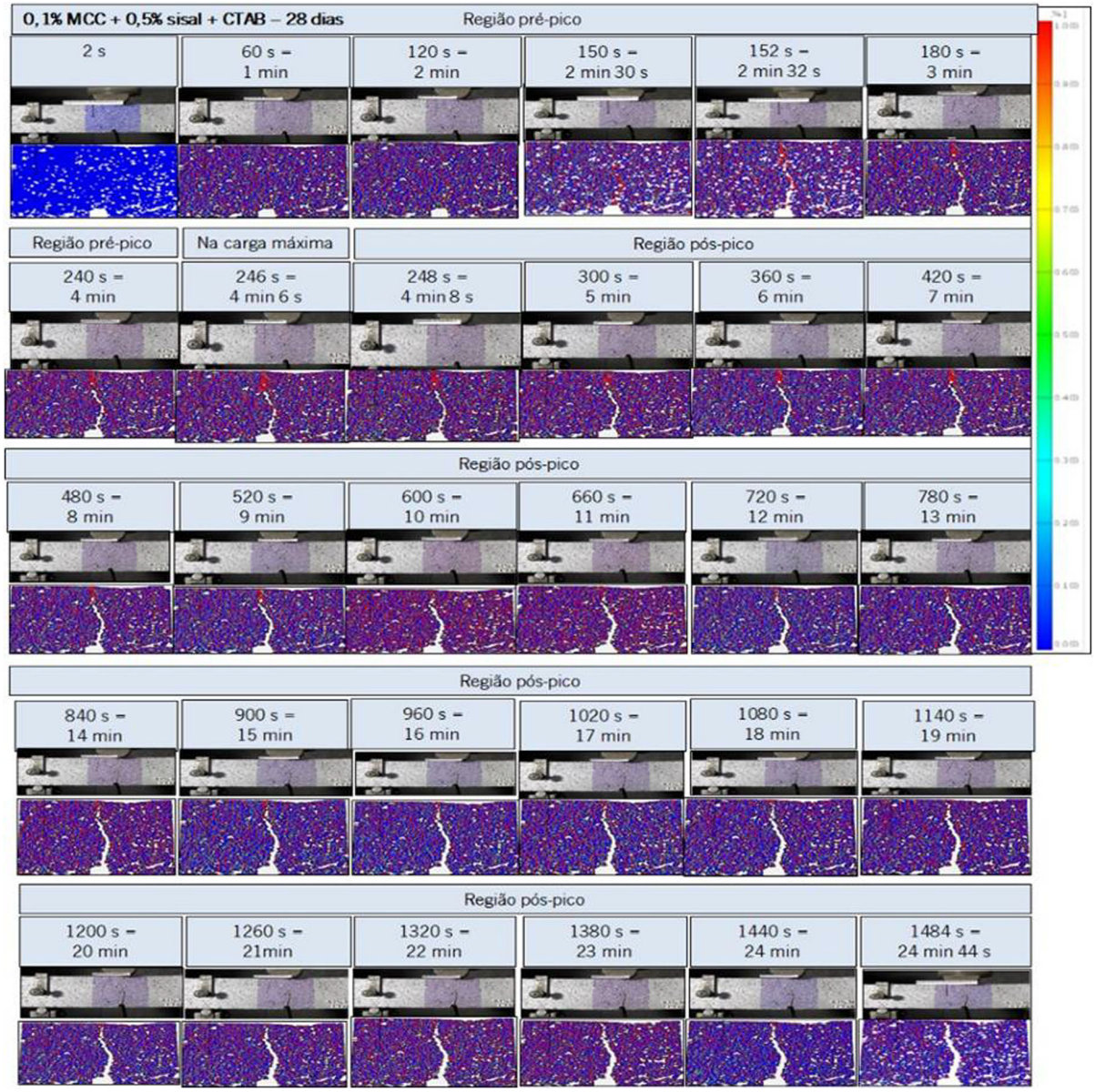

Fig. 8 Crack propagation behavior of a hierarchical composite as studied by DIC method

Table 4 Properties of the fracture - crack propagation

Samples	Time		
	Fracture initiation	At the peak load	End of the test
Plain mortar	2 min 20 s	2 min 20 s	8 min 22 s
0.5% sisal	2 min	4 min 24 s	12 min 18 s
0.1% MCC + 0.5% sisal	2 min 30 s	4 min 6 s	24 min 44 s

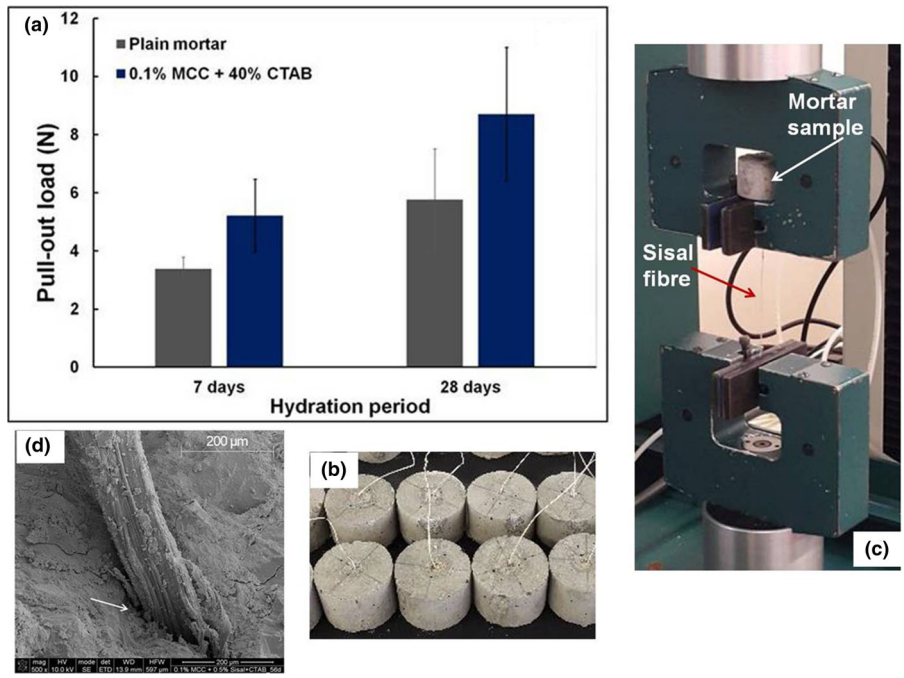

Fig. 9 Single fibre pull-out loads for plain mortar and mortar containing MCC and CTAB (**a**), samples used for pull-out testing (**b**), the pull-out test setup (**c**) and fibre-matrix bonding in hierarchical composite (**d**) [the arrow shows the bonding region of sisal fibres with cementitious matrix]

improved the microstructure of these composites. An increase in MCC concentration increased MCC agglomeration and therefore, reduced the favorable effects of MCC addition. Lower carbonation of hierarchical composites is expected to enhance their durability as carbonation is a potential cause of corrosion of steel reinforcements and resulting deterioration of concrete's mechanical properties (Chen et al. 2019).

XRD analysis of plain mortar and selected hierarchical cementitious composite (0.1% MCC + 0.50% sisal), presented in Fig. 11, further supports the observation of DTG analysis. XRD analysis characterized various products formed during the hydration process (Cao et al. 2015; Parveen et al. 2017b). The XRD spectra of both plain mortar and hierarchical composites showed the peaks for $Ca(OH)_2$ and its intensity represents the degree of hydration in the composites (Parveen et al. 2017b; Yang et al. 2017). The presence of higher intensity of $Ca(OH)_2$ peaks in hierarchical composites as compared to plain mortar indicates higher degree of hydration (Parveen et al. 2017b; Yang et al. 2017), as also observed from the DTG analysis.

Earlier studies on MCC and CNT-based and MCC-CNT hierarchical cementitious composites also reported intense $Ca(OH)_2$ peaks in the XRD spectra due to better hydration and formation of higher amount of hydration products (Parveen et al. 2015, 2017b, 2018; Alshaghel et al. 2018; Silva et al. 2018). It was also interesting to note that the peaks near 25° and 40° disappeared in the composite sample. These peaks were due to dicalcium silicate (C_2S) and tricalcium silicate (C_3S), which were present in the cement powder and underwent the hydration reaction to produce $Ca(OH)_2$ and other hydration products (Kontoleontos et al. 2013). These peaks are usually present in the XRD spectra of cement powder and disappear once hydration is complete. Therefore, the disappearance of these peaks in the composite sample indicates superior hydration and conversion of C_2S and C_3S into various hydration products, whereas their presence in the plain mortar indicates that some unreacted C_2S and C_3S were present in the plan mortar after 28 days of hydration.

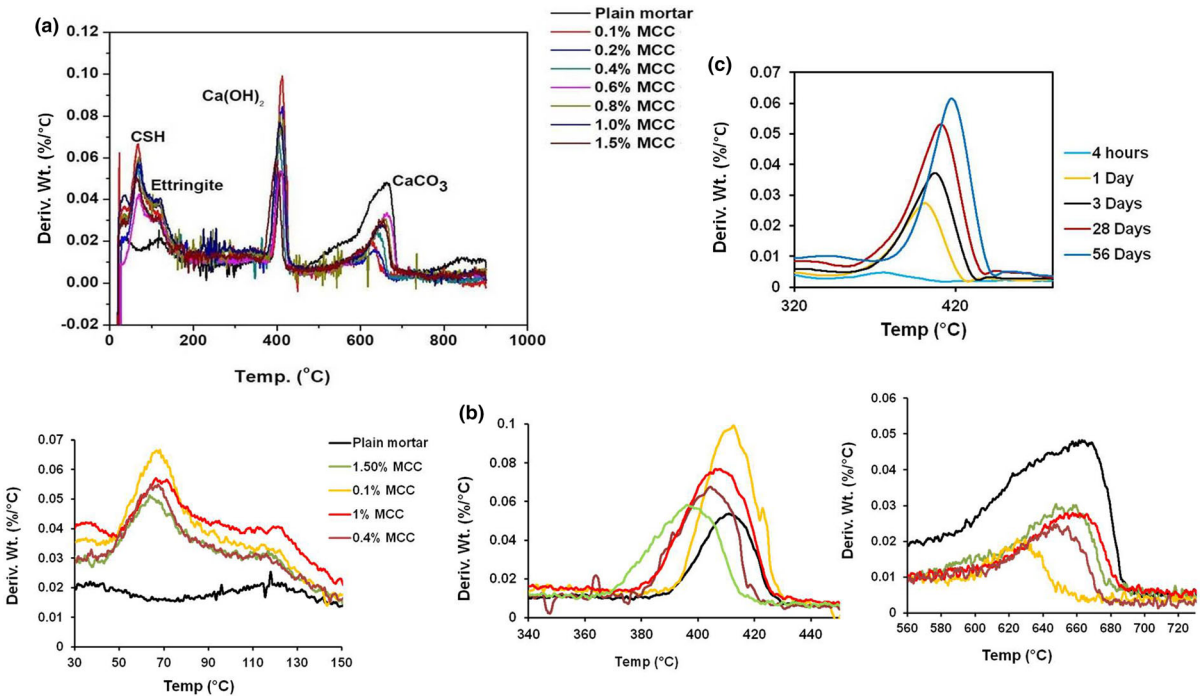

Fig. 10 DTG curves (**a**) of plain mortar and hierarchical cementitious composites with MCC (0.1–1.5%) and sisal fibers (0.50%) and enlarged views (**b**) of major DTG peaks, i.e. evaporation of water, decomposition of $Ca(OH)_2$ and decomposition of $CaCO_3$ and $Ca(OH)_2$ peaks (**c**) of hierarchical composites (0.1% MCC + 0.5% sisal) at different hydration periods

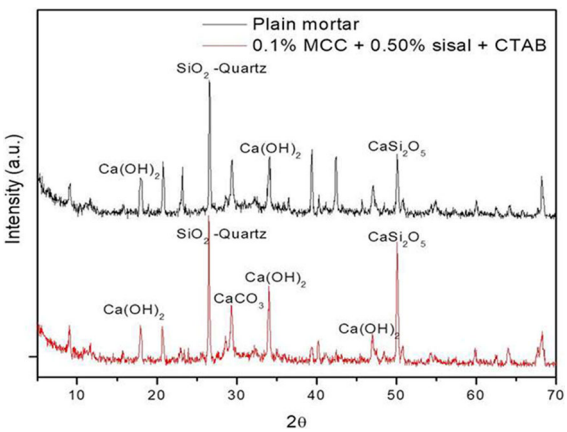

Fig. 11 XRD spectra of plain mortar and hierarchical composites

Density and porosity of plain mortar and hierarchical composites

Density, average pore size and porosity, as characterized by MIP, of plain mortar and selected hierarchical cementitious composite (0.1% MCC + 0.5% sisal) is listed in Table 5. The intruded volume of mercury in these samples is presented in Fig. 17 (Appendix). It is clear that the hierarchical composite presented a higher density along with a lower average pore size and overall porosity as compared to plain mortar. This confirmed the formation of a better microstructure in case of hierarchical composites as also confirmed from the TGA analysis. Earlier studies also reported lower average pore size in case of CNT, NCC, MCC and CNT-MCC hierarchical composites (Parveen et al. 2015, 2017b, 2018; Alshaghel et al. 2018; Silva et al. 2018; Wang et al. 2020). While due to their nano-sized structure CNTs could reduce pore size of cementitious composites by their pore-filling effect (Parveen et al. 2015; Chen et al. 2019), the formation of higher amount of hydration products was the main reason behind improved microstructure of MCC based composites (Parveen et al. 2017b, 2018). In spite of reduced pore size, an increase in the overall porosity was previously noticed in MCC based composites due to MCC agglomeration (Parveen et al. 2017b, 2018). However, the reduction of both pore size and porosity in the present study confirmed that a homogeneous

Table 5 Density of plain mortar and selected hierarchical cementitious composites

Samples	Density (g/cm^3)	Average Pore Diameter (nm)	Porosity (%)	Coefficient of water absorption $kg/(m^2\ min^{0.5})$
Plain mortar	2.39	44.1	13.7	0.065
0.1% MCC + 0.5% sisal + CTAB	2.46	34.7	12.3	0.057

MCC dispersion with negligible MCC agglomeration was achieved using CTAB at 0.1 wt% MCC.

The porosity data was further supported by the water absorption results of plain mortar and hierarchical composites listed in Table 5 and graphically presented in Fig. 12. As shown in Fig. 12a, the capillary water absorption reduced significantly over a prolonged time period (studied up to 200 $min^{0.5}$, i.e. 28 days) in hierarchical composites due to reduced porosity. The co-efficient of capillary water absorption, calculated from the slope of linear region of water absorption curve (Fig. 12b), was also higher in case of plain mortar. Therefore, addition of MCC significantly reduced the water penetration within cementitious composites.

Carbonation resistance of cementitious composites

Carbonation of concrete occurs due to penetration of atmospheric CO_2 through the capillary pores and subsequent reaction with the hydration products to form $CaCO_3$ (Cao et al. 2015). Previous studies demonstrated improved carbonation resistance of cementitious composites due to CNT addition resulting from their crack bridging effect (Carriço et al. 2018).

The carbonation resistance of plain mortar and hierarchical cementitious composites after 2, 4, 9, 14, 21, 28, 56 and 70 days of exposure periods is shown in Fig. 13. It is possible to see clearly that carbonation started in case of plain mortar within 2 days (indicated by an arrow in Fig. 13a), while in the hierarchical composite the carbonation started only after 9 days (Fig. 13b). The delayed carbonation in case of hierarchical composites was attributed to the lower average porosity and pore size, as discussed earlier, which allowed lower penetration of CO_2 into the composite. This observation is in complete agreement with the results of water absorption and $CaCO_3$ formation in DTG analysis. A refined and dense microstructure in case of hierarchical composites resulted in lower water absorption and CO_2 penetration during cement hydration as well as in the carbonation test.

Degradation of cementitious composites

The compressive strength of hierarchical composite (containing 0.1% MCC and 0.5% sisal fiber) at different ageing cycles is shown in Fig. 14a.

It can be clearly observed that there was no significant change in the compressive strength after

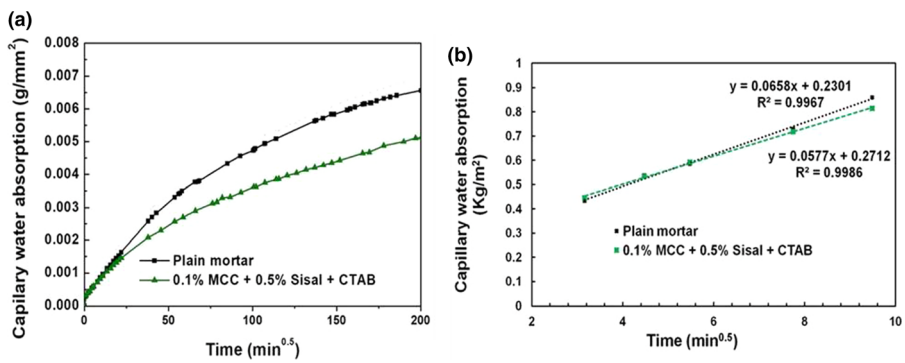

Fig. 12 Capillary water absorption of plain mortar and cementitious composites over the whole time range (**a**) and in initial linear range of the absorption curve (**b**)

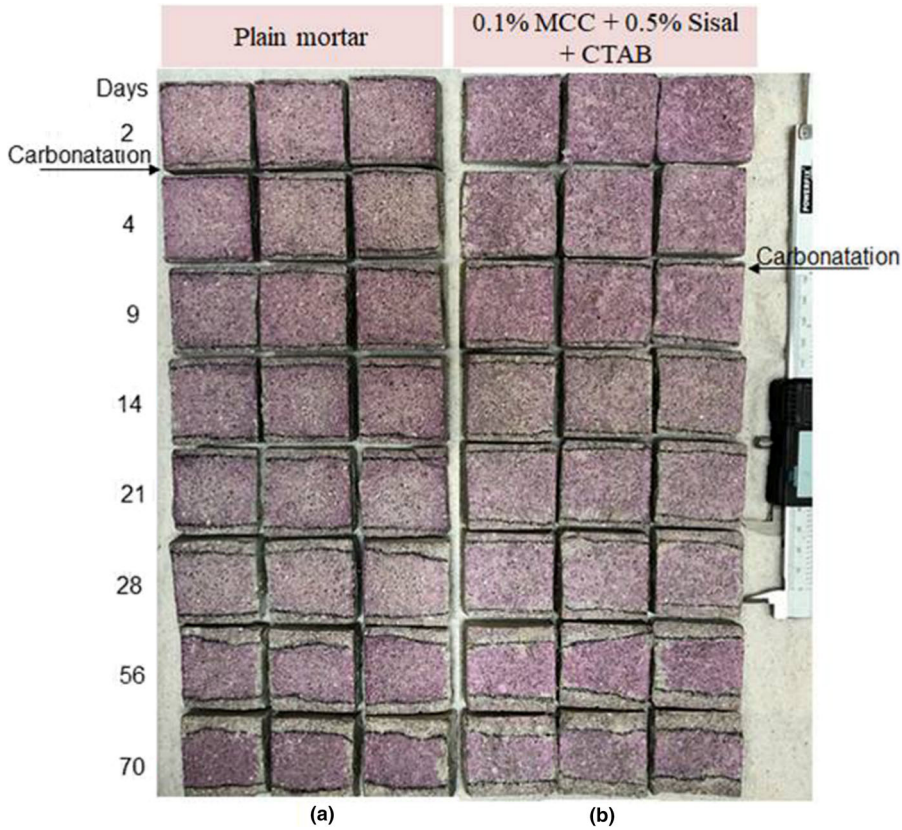

Fig. 13 Carbonation in plain mortar (**a**) and 0.1% MCC + 0.5% sisal based composites (**b**)

90 ageing cycles. A slight increase in compressive strength in the initial ageing cycles could be due to continued hydration process with time. Previous studies suggested that sisal fibers could degrade in the alkaline pH of cementitious composites (Wei and Meyer 2014; de Klerk et al. 2020) and consequently, hierarchical composites containing sisal fibers could lose their mechanical properties with degradation period. However, no strength loss in the developed hierarchical composites suggested adequate stability of sisal fibers within these composites, which has been further confirmed through FTIR and SEM studies. Figure 14b shows FTIR spectra of raw sisal fibers and sisal fibers extracted from the hierarchical composites. It can be noticed that the sisal fibers embedded in the composite showed identical characteristics peaks (e.g. 3700–3000 cm^{-1} for OH group, 2924 cm^{-1} due C-H stretching in cellulose and hemicellulose, 1732 cm^{-1} stretching of carboxyl and acetyl groups in hemicellulose and lignin, 1605 cm^{-1} due to aromatic groups in lignin, 1238 cm^{-1} due to acetyl groups in hemicellulose and aryl group in lignin, 1030 cm^{-1} attributed to C-O stretching in lignin, etc.), as also observed in case of raw sisal fibers (Fernandes et al. 2013). This confirmed that the sisal fibers were not degraded and their chemical structure was intact after 90 ageing cycles. Figure 14c shows the morphology of sisal fibers after different ageing periods. It can be observed that sisal fibers maintained similar morphology after the aging period without any noticeable physical damage. Earlier studies demonstrated the ability of coated nanocellulose in reducing fiber mineralization (through reduction in the penetration of alkaline ions into the plant fiber structure) and degradation in cementitious matrices (Mohammadkazemi et al. 2015), which was also achieved with MCC in the present study. All these observations suggested that the developed hierarchical composites have adequate durability for using them in construction applications.

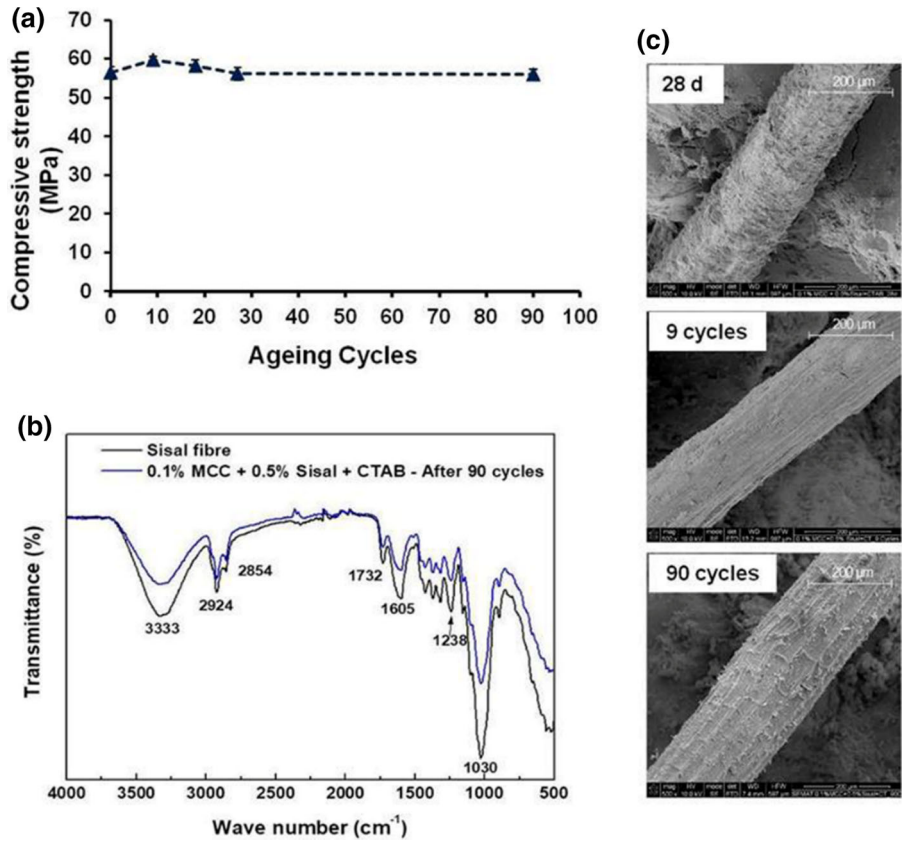

Fig. 14 Durability study of developed hierarchical composites showing the effect of degradation cycle on (**a**) change in compressive strength (**b**) chemical structure and (**c**) physical surface morphology

Conclusions

In this work, new hierarchical cementitious composites were developed using short sisal fibers (20 mm, 0.25 and 0.5 wt% of cement) and MCC (0.1–1.5 wt%) using CTAB as the dispersing agent and characterized for MCC dispersion, flow behavior of mortar paste, density, porosity, hydration products, mechanical properties, carbonation resistance and durability of cementitious composites. Following conclusions were made from this study:

- MCC aqueous suspensions showed increased agglomeration and reduced stability with increase in MCC concentration. The optimum MCC dispersion was achieved with 40% CTAB (on the weight of MCC), which was used for the fabrication of cementitious composites.
- Among MCC and sisal fibers, MCC showed higher influence on the flow properties of mortar paste due to their higher surface area and moisture absorption property. At the same sisal fiber content flow properties of fresh mortar first decreased up to 0.2% MCC due to rapid water absorption by MCC, then increased up to 0.8% MCC mainly due to increased amount of CTAB used and after that it started to decrease again due to severe MCC agglomeration. Also, a CTAB: TBP ratio of 1:1 was found to be optimum to suppress foam formation and reduce porosity in cementitious composites.
- In hierarchical composites, compressive and flexural strengths improved significantly at 0.1 wt% MCC and further increase in MCC concentration reduced mechanical strengths drastically due to MCC agglomeration. Although the effect of sisal fibers on compressive strength was not positive, an increase in sisal fiber content in hierarchical composites from 0.25 to 0.5 wt% resulted in an improved flexural strength mainly due to crack-

bridging effect of sisal fibers. Hierarchical composites containing 0.1% MCC with 0.5% sisal fibers showed ~ 24% and 18% higher flexural and compressive strengths, respectively as compared to plain mortar.

- Hierarchical scale composites showed a synergistic effect on the fracture behavior resulting in a slower crack initiation and propagation as compared to both sisal fiber-reinforced and plain mortar composites. The fracture energy of hierarchical composites improved by 40% as compared to plain mortar composites. Hierarchical composites also demonstrated superior sisal fiber-matrix bonding due to positive influence of MCC on composite's interface.
- Hierarchical composites showed formation of a higher amount of hydration products as confirmed from the DTG and XRD analyses. As a result, a decrease in porosity and average pore size accompanied by an increase in density was observed in hierarchical composites. The lower porosity of hierarchical composites reduced the water absorption and penetration of CO_2, resulting in an increase in the carbonation resistance. The hierarchical composites were also durable without any noticeable damage to the sisal fibers up to 90 accelerated ageing cycles.

Therefore, the developed new hierarchical cementitious composites containing MCC and sisal fibers hold great promise in construction applications due to their superior mechanical strengths, fracture energy and durability, besides they can be manufactured using low-cost, renewable and eco-friendly plant-based raw materials.

Acknowledgments The authors gratefully acknowledge the funding by Araucária Foundation to Support Scientific and Technological Development of the State of Paraná under grants CP20/2013, Department of Civil Engineering of Apucarana Campus—Federal University of Technology—Paraná (UTFPR), State University of Maringá (UEM)—Brazil, Fibernamics, Fibrous Materials Research Group and University of Minho—Guimarães, Portugal, Project UID/CTM/00264/2019 of 2C2T—Centro de Ciência e Tecnologia Têxtil, funded by National Founds through FCT/MCTES and University Beira Interior—Covilhã, Portugal.

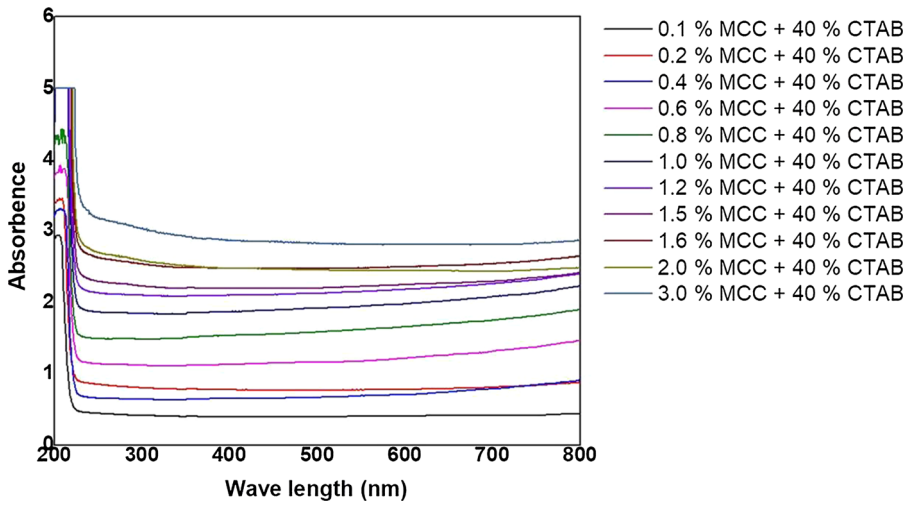

Fig. 15 UV-Vis spectra of MCC aqueous suspensions prepared using 40% CTAB

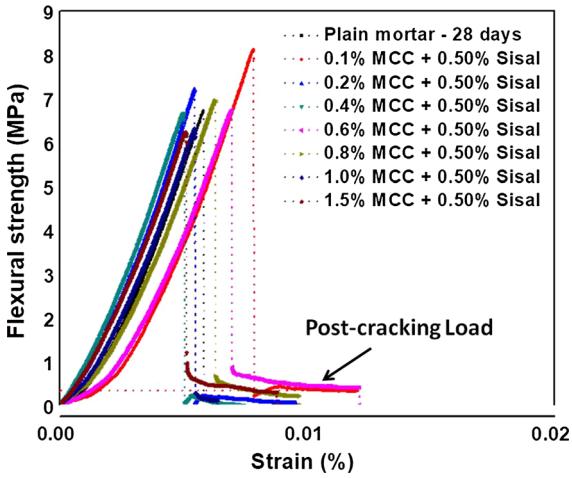

Fig. 16 Flexural stress-stain curves of plain mortar and selected hierarchical composites, demonstrating the post-cracking load-carrying ability of sisal fibers

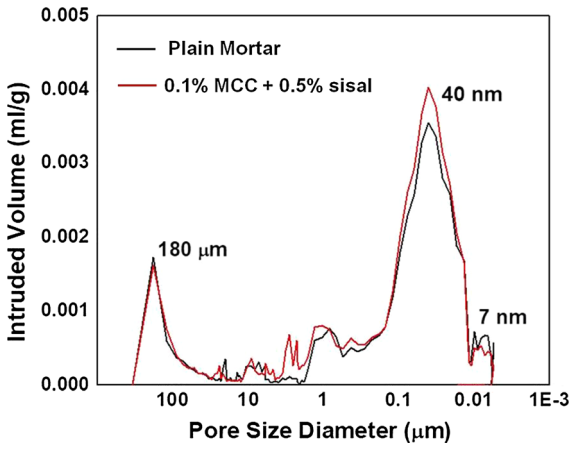

Fig. 17 Intruded volume of mercury in plain mortar and hierarchical cementitious composites containing 0.1% MCC and 0.5% sisal fibers

Data availability The raw/processed data required to reproduce these findings cannot be shared at this time as the data also forms part of an ongoing study. The relevant data can be made available on request.

Appendix

See Figs. 15, 16 and 17.

References

Alrekabi S, Cundy AB, Lampropoulos A et al (2017) Mechanical performance of novel cement-based composites prepared with nano-fibers, and hybrid nano-and micro-fibers. Compos Struct 178:145–156

Alshaghel A, Parveen S, Rana S, Fangueiro R (2018) Effect of multiscale reinforcement on the mechanical properties and microstructure of microcrystalline cellulose-carbon nanotube reinforced cementitious composites. Compos Part B Eng 149:122–134

Anju TR, Ramamurthy K, Dhamodharan R (2016) Surface modified microcrystalline cellulose from cotton as a potential mineral admixture in cement mortar composite. Cem Concr Compos 74:147–153. https://doi.org/10.1016/j.cemconcomp.2016.09.003

Balea A, Fuente E, Blanco A, Negro C (2019) Nanocelluloses: Natural-based materials for fiber-reinforced cement composites. A critical review. Polymers (Basel) 11

Brandt AM (2008) Fibre reinforced cement-based (FRC) composites after over 40 years of development in building and civil engineering. Compos Struct 86:3–9. https://doi.org/10.1016/j.compstruct.2008.03.006

Cao Y, Zavaterri P, Youngblood J et al (2015) The influence of cellulose nanocrystal additions on the performance of cement paste. Cem Concr Compos 56:73–83. https://doi.org/10.1016/j.cemconcomp.2014.11.008

Cao M, Xie C, Guan J (2019) Fracture behavior of cement mortar reinforced by hybrid composite fiber consisting of CaCO 3 whiskers and PVA-steel hybrid fibers. Compos Part A Appl Sci Manuf 120:172–187. https://doi.org/10.1016/j.compositesa.2019.03.002

Carriço A, Bogas JA, Hawreen A, Guedes M (2018) Durability of multi-walled carbon nanotube reinforced concrete. Constr Build Mater 164:121–133. https://doi.org/10.1016/j.conbuildmat.2017.12.221

Chen Z, Lee Y, Cho H et al (2019) Improvement in carbonation resistance of portland cement mortar incorporating γ -dicalcium silicate. Adv Mater Sci Eng. https://doi.org/10.1155/2019/9856734

Clark MD, Subramanian S, Krishnamoorti R (2011) Understanding surfactant aided aqueous dispersion of multi-walled carbon nanotubes. J Colloid Interface Sci 354:144–151. https://doi.org/10.1016/J.JCIS.2010.10.027

Das K, Ray D, Bandyopadhyay NR et al (2009) A study of the mechanical, thermal and morphological properties of microcrystalline cellulose particles prepared from cotton slivers using different acid concentrations. Cellulose 16:783–793. https://doi.org/10.1007/s10570-009-9280-6

de Klerk MD, Kayondo M, Moelich GM et al (2020) Durability of chemically modified sisal fibre in cement-based composites. Constr Build Mater. https://doi.org/10.1016/j.conbuildmat.2019.117835

Eyley S, Thielemans W (2014) Surface modification of cellulose nanocrystals. Nanoscale 6:7764–7779. https://doi.org/10.1039/c4nr01756k

Fan M, Fu F (2016) Advanced high strength natural fibre composites in construction

Fernandes EM, Mano JF, Reis RL (2013) Hybrid cork-polymer composites containing sisal fibre: morphology, effect of the

fibre treatment on the mechanical properties and tensile failure prediction. Compos Struct 105:153–162. https://doi.org/10.1016/j.compstruct.2013.05.012

Fu T, Moon RJ, Zavattieri P, et al (2017) Cellulose nanomaterials as additives for cementitious materials. In: Cellulose-reinforced nanofibre composites: production, properties and applications. Elsevier Ltd, pp 455–482

Fujiyama R, Darwish F, Pereira MV (2014) Mechanical characterization of sisal reinforced cement mortar. Theor Appl Mech Lett 4:061002. https://doi.org/10.1063/2.1406102

Gómez Hoyos C, Cristia E, Vázquez A (2013) Effect of cellulose microcrystalline particles on properties of cement based composites. Mater Des 51:810–818. https://doi.org/10.1016/j.matdes.2013.04.060

Haddad Kolour H, Ashraf W, Landis EN (2020) Hydration and early age properties of cement pastes modified with cellulose nanofibrils. Transp Res Rec J Transp Res Board. https://doi.org/10.1177/0361198120945993

Hisseine OA, Wilson W, Sorelli L et al (2019) Nanocellulose for improved concrete performance: a macro-to-micro investigation for disclosing the effects of cellulose filaments on strength of cement systems. Constr Build Mater 206:84–96. https://doi.org/10.1016/j.conbuildmat.2019.02.042

International Energy Agency (2020) Cement—analysis—IEA. https://www.iea.org/reports/cement. Accessed 24 Aug 2020

Kontoleontos F, Tsakiridis P, Marinos A et al (2013) Dry-grinded ultrafine cements hydration. Physicochemical and microstructural characterization. Mater Res 16:404–416. https://doi.org/10.1590/S1516-14392013005000014

Lima PRL, Santos HM, Camilloto GP, Cruz RS (2017) Effect of surface biopolymeric treatment on sisal fiber properties and fiber-cement bond. J Eng Fiber Fabr 12:59–71. https://doi.org/10.1177/155892501701200207

Liu W, Fei M, Ban Y et al (2017) Preparation and evaluation of green composites from microcrystalline cellulose and a soybean-oil derivative. Polymers (Basel) 9:541. https://doi.org/10.3390/polym9100541

Metaxa ZS, Konsta-Gdoutos MS, Shah SP (2010) Mechanical properties and nanostructure of cement-based materials reinforced with carbon nanofibers and Polyvinyl Alcohol (PVA) microfibers. In: American Concrete Institute, ACI Special Publication. pp 115–126

Mohammadkazemi F, Doosthoseini K, Ganjian E, Azin M (2015) Manufacturing of bacterial nano-cellulose reinforced fiber-cement composites. Constr Build Mater 101:958–964. https://doi.org/10.1016/j.conbuildmat.2015.10.093

Mohan Bhasney S, Kumar A, Katiyar V (2020) Microcrystalline cellulose, polylactic acid and polypropylene biocomposites and its morphological, mechanical, thermal and rheological properties. Compos Part B Eng. https://doi.org/10.1016/j.compositesb.2019.107717

Onésippe C, Passe-Coutrin N, Toro F et al (2010) Sugar cane bagasse fibers reinforced cement composites: thermal considerations. Compos Part A Appl Sci Manuf 41:549–556. https://doi.org/10.1016/j.compositesa.2010.01.002

Parveen S, Rana S, Fangueiro R, Paiva MC (2015) Microstructure and mechanical properties of carbon nanotube reinforced cementitious composites developed using a novel dispersion technique. Cem Concr Res 73:215–227. https://doi.org/10.1016/J.CEMCONRES.2015.03.006

Parveen S, Rana S, Fangueiro R (2017a) Macro- and nanodimensional plant fiber reinforcements for cementitious composites. In: Sustainable and nonconventional construction materials using inorganic bonded fiber composites. Elsevier, pp 344–382

Parveen S, Rana S, Fangueiro R, Paiva MC (2017b) A novel approach of developing micro crystalline cellulose reinforced cementitious composites with enhanced microstructure and mechanical performance. Cem Concr Compos 78:146–161. https://doi.org/10.1016/j.cemconcomp.2017.01.004

Parveen S, Rana S, Ferreira S et al (2018) Ultrasonic dispersion of micro crystalline cellulose for developing cementitious composites with excellent strength and stiffness. Ind Crops Prod 122:156–165. https://doi.org/10.1016/j.indcrop.2018.05.060

Pichandi S, Rana S, Parveen S, Fangueiro R (2018) A green approach of improving interface and performance of plant fibre composites using microcrystalline cellulose. Carbohydr Polym 197:137–146. https://doi.org/10.1016/j.carbpol.2018.05.074

Rastogi R, Kaushal R, Tripathi SK et al (2008) Comparative study of carbon nanotube dispersion using surfactants. J Colloid Interface Sci 328:421–428. https://doi.org/10.1016/j.jcis.2008.09.015

Rehman MM, Zeeshan M, Shaker K, Nawab Y (2019) Effect of micro-crystalline cellulose particles on mechanical properties of alkaline treated jute fabric reinforced green epoxy composite. Cellulose 26:9057–9069. https://doi.org/10.1007/s10570-019-02679-4

Savastano H, Santos SF, Radonjic M, Soboyejo WO (2009) Fracture and fatigue of natural fiber-reinforced cementitious composites. Cem Concr Compos 31:232–243. https://doi.org/10.1016/j.cemconcomp.2009.02.006

Silva FA, Mobasher B, Filho RDT (2009) Cracking mechanisms in durable sisal fiber reinforced cement composites. Cem Concr Compos 31:721–730. https://doi.org/10.1016/j.cemconcomp.2009.07.004

Silva L, Parveen S, Filho A et al (2018) A facile approach of developing micro crystalline cellulose reinforced cementitious composites with improved microstructure and mechanical performance. Powder Technol. https://doi.org/10.1016/j.powtec.2018.07.076

Swolfs Y, Gorbatikh L, Verpoest I (2014) Fibre hybridisation in polymer composites: a review. Compos. Part A Appl Sci Manuf 67:181–200

Tarchoun AF, Trache D, Klapötke TM et al (2019) Ecofriendly isolation and characterization of microcrystalline cellulose from giant reed using various acidic media. Cellulose 26:7635–7651. https://doi.org/10.1007/s10570-019-02672-x

Wang J, Tao J, Li L et al (2020) Thinner fillers, coarser pores? A comparative study of the pore structure alterations of cement composites by graphene oxides and graphene nanoplatelets. Compos Part A Appl Sci Manuf 130:105750. https://doi.org/10.1016/j.compositesa.2019.105750

Wei J, Meyer C (2014) Improving degradation resistance of sisal fiber in concrete through fiber surface treatment. Appl Surf Sci 289:511–523. https://doi.org/10.1016/j.apsusc.2013.11.024

Yang H, Monasterio M, Cui H, Han N (2017) Experimental study of the effects of graphene oxide on microstructure and properties of cement paste composite. Compos Part A Appl Sci Manuf 102:263–272. https://doi.org/10.1016/j.compositesa.2017.07.022